Aging and Disease
www.aginganddisease.org
Early access date: June 19, 2025
http://dx.doi.org/10.14336/AD.2025.0507

Original Article

Astrocytic Glucose Sensing Drives Synaptic Depression under Metabolic Stress

Andrés M. Baraibar[1,2,3,4#], Carlos G. Ardanaz[5,6#], Susana Mato[1,2,3], Paulo Kofuji[4], Alfonso Araque[4*], Maite Solas[5,6*]

[1]Department of Neurosciences, University of the Basque Country UPV/EHU, 48940 Leioa, Spain. [2]Achucarro Basque Center for Neuroscience, 48940 Leioa, Spain. [3]Neuroinmunology Group, Biobizkaia Health Research Institute, 48903 Barakaldo, Spain. [4]Department of Neuroscience, University of Minnesota, Minneapolis, 55455 MN, USA. [5]Department of Pharmaceutical Sciences, Division of Pharmacology, University of Navarra, 31008 Pamplona, Spain. [6]IdiSNA, Navarra Institute for Health Research, 31008 Pamplona, Spain.

[Received April 15, 2025; Revised June 9, 2025; Accepted June 10, 2025]

ABSTRACT: Glucose is the primary energy source for the brain, and its continuous supply is essential for neuronal function. Astrocytes play a pivotal role in brain energy metabolism by mediating glucose uptake, sensing metabolic fluctuations, and modulating synaptic activity. However, astrocyte responses to transient glucose deprivation remain incompletely understood. Here, we demonstrate that astrocytic glucose uptake is crucial for network adaptation to metabolic stress. Using electrophysiology and calcium imaging approaches, we show that glucose deprivation depresses hippocampal synaptic transmission through an astrocyte-dependent mechanism that involves decreased glucose transporter 1 (GLUT1)-facilitated extracellular glucose uptake, intracellular calcium elevations, and ATP/adenosine-mediated signaling, which leads to excitatory neurotransmission depression via A1 receptors. Moreover, astrocyte-specific GLUT1 depletion prevents astrocytic responses to glucose deprivation and precludes the effects of glucose deprivation on synaptic transmission, thereby indicating that GLUT1-dependent glucose uptake is involved in astrocyte-mediated modulation of synaptic function. These findings extend the concept of astrocytic metabolic regulation beyond regions canonically classified as glucose-sensing and establish astrocytes as key integrators of energy availability and synaptic function. Our study provides new insights into the role of astrocytes in brain energy homeostasis and identifies potential therapeutic targets for metabolic disorders affecting the nervous system.

Key words: Astrocytes, GLUT1, metabolic stress, synaptic depression, calcium signaling

INTRODUCTION

Astrocytes play fundamental roles in brain homeostasis by providing metabolic substrates to neurons in an activity-dependent manner [1]. Glucose is a major primary energy source for brain function, and astrocytes ensure its uptake, distribution and need-based utilization [2]. These cells facilitate the uptake of glucose from the bloodstream through glucose transporter-1 (GLUT1) expressed at the astrocytic perivascular endfeet [3–5], and subsequently metabolize it into lactate, which is then delivered to neurons to be used as energy substrate [1, 6]. This astrocyte-to-neuron metabolic coupling is essential in sustaining synaptic activity and neuronal function [7].

Besides their well-established function as key mediators of brain neuroenergetics, astrocytes are active participants in synaptic function. Astroglial cells respond to synaptically-released neurotransmitters with intracellular calcium (Ca^{2+}) elevations that result in the release of gliotransmitters — mainly glutamate, ATP and D-serine — which in turn modulates neuronal network activity in a tightly controlled manner [8–10]. Astrocytes

***Correspondence should be addressed to:** Dr. Alfonso Araque, University of Minnesota, Minneapolis, MN 55455, USA. Email: araque@umn.edu and Dr. Maite Solas, Division of Pharmacology, University of Navarra, Pamplona, 31008, Spain. Email: msolaszu@unav.es. #These authors contributed equally.

are thus functionally well-poised to participate in the modulation of synaptic function induced by glucose deprivation. However, the molecular mechanisms that underlie astrocyte metabolic supply, as well as their impact on synaptic transmission, remain incompletely understood.

The brain exhibits a high rate of glucose consumption but its access to this essential energy source is limited, as glucose cannot be locally synthesized or stored in substantial amounts as glycogen [11–14]. Consequently, the brain is highly susceptible to fluctuations in blood glucose supply, which can impair neuronal function [15–18]. Glucose deprivation may occur under sustained neuronal activity when brain energy demand exceeds supply, fasting, or pathological states such as ischemia and diabetes. Moreover, aging-associated cognitive decline and memory impairments linked to recurrent hypoglycemic episodes have been proposed to be mediated by glucose deficits [19–24].

Glucose deprivation is known to induce a slow and reversible depression of excitatory synaptic transmission [25–27], but whether this phenomenon is due to decreased neuronal energy availability or to neurotransmitter- or gliotransmitter-mediated signaling remains controversial. On mechanistic grounds, oxygen and/or glucose deprivation depress hippocampal synaptic transmission through adenosine signaling and activation of A1 receptors (A1Rs) [27]. However, the cellular origin of the adenosine mediating excitatory synaptic depression in low-glucose conditions is yet to be deciphered.

In this study, we combined electrophysiology and Ca^{2+} imaging techniques, as well as transgenic mouse models with astrocytic GLUT1 depletion, to investigate the contribution of astrocytes to synaptic depression under metabolic stress. We found that glucose deprivation induces hippocampal synaptic depression through an astrocyte-dependent mechanism that involves decreased GLUT1-mediated glucose uptake, intracellular calcium signaling, ATP release and its extracellular conversion to adenosine by ectonucleotidases, ultimately leading to the suppression of excitatory neurotransmission via A1 receptors. These findings shed light on the molecular mechanisms that underline astrocyte-mediated modulation of neuroenergetics and synaptic function in glucose-deprived conditions, potentially revealing novel therapeutic targets for metabolic and neurodegenerative disorders.

MATERIALS AND METHODS

Ethics statement

All of the procedures for handling and sacrificing animals were approved by the University of Minnesota Institutional Animal Care and Use Committee (IACUC) in compliance with the National Institutes of Health guidelines for the care and use of laboratory animals, as well as, following the European and Spanish regulations (2003/65/EC; 1201/2005) for the care and use of laboratory animals and approved by the ethical committee of the University of Navarra (ethical protocol number 076-19).

Animals

Adult mice (≥ 8 weeks) were housed under 12/12-h light/dark cycle, up to 5 animals per cage, at temperatures between 22 and 24ºC at 30-70% humidity with available food and water. The following animals (males and females) were used for the present study: $IP_3R_2^{-/-}$ (generously donated by Dr J Chen) and GLUT1 floxed ($GLUT1^{fl/fl}$, Jackson Laboratories, stock number 031871).

Acute hippocampal slice electrophysiology

Mice were euthanized by decapitation and brains were rapidly removed and placed in ice-cold artificial cerebrospinal fluid ACSF (containing in mM: NaCl 124, KCl 5, NaH_2PO_4 1.25, $MgSO_4$ 2, $NaHCO_3$ 26, $CaCl_2$ 2, glucose 10; gassed with 95% O_2, 5% CO_2, and maintained between pH 7.3 and 7.4). 350-µm-thick coronal brain slices containing the hippocampus were obtained in a 4ºC ACSF solution using a Leica VT1200 vibratome. Following cutting, slices were allowed to recover in ACSF for 30 min at 31ºC followed by 30 min at 20-22ºC before recording. After a 1-h recovery period, slices were kept at 20–22ºC for the rest of the recording day. Slices were then transferred to an immersion recording chamber and superfused at 2 mL/min with gassed ACSF kept at 34ºC with a temperature controller TC-324B (Warner Instruments Co.). Cells were visualized using infrared-differential interference contrast optics (Nikon Eclipse E600FN, Tokyo, Japan) and a 40x water immersion lens. CA1 hippocampal subfields were identified with a 10x objective. Transient glucose deprivation episodes were induced by switching the perfusion from normal ACSF to 0 glucose ACSF (containing in mM: NaCl 134, KCl 5, NaH_2PO_4 1.25, $MgSO_4$ 2, $NaHCO_3$ 26, $CaCl_2$ 2) typically for 10 min.

To study excitatory postsynaptic currents (EPSCs), picrotoxin (50 µM) and CGP54626 (1 µM) were added to the solution to block GABA-A and GABA-B receptors, respectively. Whole-cell electrophysiological recordings were obtained from hippocampal CA1 pyramidal neurons using patch electrodes (3-10 MΩ) filled with an internal solution containing (in mM): KGluconate 135, KCl 10, HEPES 10, $MgCl_2$ 1, ATP-Na_2 2 (pH = 7.3). For some experiments astrocytes were patched with 4-9 MΩ

electrodes filled with an intracellular solution containing (in mM): $MgCl_2$ 1, NaCl 8, ATP-Na_2 2, GTP 0.4, HEPES 10, and 20 mM BAPTA, titrated with KOH to pH 7.2-7.3 and including Alexa 594 (100 µM) to visualize the astrocyte syncytium. Recordings were performed using MultiClamp 700B amplifier (Molecular Devices, San Jose, CA). Fast and slow whole-cell capacitances were neutralized, series resistance was compensated (~70%), and the membrane potential was held at -70 mV. Intrinsic electrophysiological properties were monitored at the beginning and the end of the experiments. Series and input resistances were monitored throughout the experiment using a -5 mV pulse. Recordings were considered stable when the series and input resistances, membrane resistance, and duration of the stimulus artifact did not change >20% and I–V curves and firing patterns at the beginning and the end of the experiments were similar. Recordings that did not meet these criteria were discarded. Signals were filtered at 1 kHz, acquired at a 10 kHz sampling rate, and fed to a Digidata 1322A digitizer (Molecular Devices; San Jose, CA, USA). pCLAMP 10.3 (Axon Instruments, Molecular Devices; San Jose, CA, USA) was used for stimulus generation, data display, data acquisition, and data storage. Evoked EPSCs were recorded using theta capillaries (2–5 µm tip) filled with ACSF for bipolar stimulation. The electrodes were connected to a stimulator S-900 through an isolation unit (Dagan Corporation, MN) and placed in the *stratum radiatum* to stimulate Schaffer collaterals. Input-output curves of EPSCs were performed by increasing stimulus intensities from 0 to 100 µA. Paired-pulse facilitation was induced by applying paired pulses with 25, 50, 75, 100, 200, 300, and 500 ms inter-pulse intervals. The paired-pulse ratio (PPR) was calculated as the relative change in EPSC amplitude, using the formula: PPR = (EPSC-2 – EPSC-1) / EPSC-1. Synaptic fatigue was assessed by applying 15 consecutive stimuli in 25 ms intervals.

AAV stereotaxic surgeries

Animals were anesthetized using a ketamine (10 mg/mL) xylazine (1 mg/mL) mixture and placed on a heating pad to maintain body temperature with faux tears applied to the cornea. Mice were placed in a stereotaxic apparatus, an incision was made down the midline of the scalp to expose the skull and bilateral intrahippocampal injections were performed at 100 nL/min using the following stereotaxic coordinates (relative to Bregma in mm): −2.3 A-P, ± 1.5 M-L and −1.2 D-V (Paxinos and Franklin 2012). Mice were then sutured and left to heal for 3 weeks. AAV5-pZac2.1-gfaABC1d-cyto-GCaMP6f (Addgene) and AAV8-GFAP-mCherry-Cre (UMN vector core) viral constructs were used. $GLUT1^{fl/fl}$ mice were injected with AAV8-GFAP-mCherry-Cre in parallel to deplete GLUT1 from astrocytes ($aGLUT1^{-/-}$ condition). Virus titers were between 10^{10} and 10^{12} genomic copies per ml for all batches of virus used in the study and were injected bilaterally at 500 nL. When more than one virus was used, they were mixed and injected at 500 nL.

Ca^{2+} imaging

GCaMP6f-dependent fluorescent Ca^{2+} signal imaging was performed using an Olympus BX51WI confocal laser scanning microscope (Olympus Optical, Japan) controlled by the ThorImageLS 4.0 software (ThorLabs, USA). Coronal slices containing the hippocampus were obtained from $GLUT1^{fl/fl}$ mice injected with AAV5-pZac2.1-gfaABC1d-cyto-GCaMP6f or with both AAV5-pZac2.1-gfaABC1d-cyto-GCaMP6f and AAV8-GFAP-mCherry-Cre in the hippocampal CA1 region (see "AAV stereotaxic surgeries" section). Ca^{2+} imaging experiments were performed superfusing slices in presence of 50 µM picrotoxin and 1 µM CGP5462 to block GABA-A and GABA-B receptors, respectively. Astrocytes within CA1 *stratum radiatum* were visualized using a 40x immersion objective and a 470 nm laser (ThorLabs, #M470F3). Videos were obtained at a 512 x 512 resolution with a sampling interval of 2 s. A custom MATLAB program (Calsee: www.araquelab.com/code/) was used to quantify fluorescence level measurements in astrocytes. Ca^{2+} variations recorded at the soma and processes of the cells were estimated as changes of the fluorescence signal over baseline ($\Delta F/F_0$), and cells were considered to show a Ca^{2+} event when the $\Delta F/F_0$ increase was at least 2 times the standard deviation of the baseline.

The astrocyte Ca^{2+} signal was quantified from the Ca^{2+} event probability, which was defined as the probability that an astrocyte in a given field of view shows Ca^{2+} elevations during a 10-sec bin. Experiments were conducted recording from 8 to 30 astrocytes per field of view. The time of occurrence was considered at the onset of the Ca^{2+} event. For each astrocyte analyzed, values of 0 and 1 were assigned for bins showing either no response or a Ca^{2+} event, respectively, and the Ca^{2+} event probability was obtained by dividing the number of astrocytes showing an event at each time bin by the total number of monitored astrocytes [28]. The Ca^{2+} event probability was calculated in each slice, and for statistical analysis, the sample size corresponded to the number of slices as different slices were considered as independent variables. The half-width of the events was also computed and averaged per 2 min. All the astrocytes that showed a Ca^{2+} event during the experiment were used for the analysis. Imaging was performed in alternating 2-minute imaging periods and 2-minute non-imaging periods to prevent photobleaching.

To assess differences in Ca^{2+} event probability under various conditions, the basal Ca^{2+} event probability (over 2 min) was averaged and compared with the average Ca^{2+} event probability during the last 2 min following 10 min of no-glucose ACSF bath application.

Immunohistochemistry

The animals were anesthetized with Avertin (2,2,2 tribromoethanol, 240 mg/kg, i.p.) and intracardially perfused with ice cold phosphate buffered saline (PBS) followed by 4% paraformaldehyde (PFA) in 0.1 M PBS (pH 7.4). The brain was removed, and 100-µm coronal sections were obtained using a Leica VT1000S vibratome. Tissue sections were incubated in blocking buffer (0.1% Triton X-100, 10% goat serum in PBS) for 1 h at room temperature and subsequently incubated for 2 days at 4°C with mouse anti-GFAP (1:500; Cell Signaling Technology, #3670) and rabbit anti-RFP (1:500; Rockland, #600-401-379) diluted in blocking solution. The slices were then washed 3 times for 15 min each in PBS and incubated with secondary antibodies diluted in PBS containing 0.1% Triton X-100 and 5% goat serum for 2 days at room temperature. The following secondary antibodies were used: goat anti-mouse IgG AlexaFluor™ 647 (1:1000; Invitrogen, #A21235) and goat anti-rabbit AlexaFluor™ 594 (1:1000; Invitrogen, #A11012). Tissue sections were then washed 3 times with PBS for 10 min each and mounted using Vectashield Mounting media (Vector laboratories). Slides were imaged using a Leica SP5 multiphoton confocal microscope and Olympus FluoView FV1000.

Drugs and chemicals

[S-(R∗,R∗)]-[3-[[1-(3,4-Dichlorophenyl)ethyl]amino]-2-hydroxypropyl](cyclohexylmethyl) phosphinic acid (CGP 54626 hydrochloride), D-(−)-2-Amino-5-phosphonopentanoic acid (D-AP5), 6-Cyano-7-nitroquinoxaline-2,3-dione disodium (CNQX disodium salt), Octahydro-12-(hydroxymethyl)-2-imino-5,9:7,10a-dimethano-10aH-[1,3]dioxocino[6,5-d], 6-*N*,*N*-Diethyl-D-β,γ-dibromomethyleneATP trisodium salt (ARL 67156 trisodium salt), 1,2-bis(2-aminophenoxy)ethane-*N*,*N*,*N*′,*N*′-tetraacetate (BAPTA), were purchased from Tocris Bioscience. Picrotoxin, from Indofine Chemical Company (Hillsborough, NJ). 9-β-D-Ribofurano-syladenine (Adenosine), 8-Cyclopentyl-1,3-dimethyl-xanthine (CPT), dipyridamole (DPM) and *S*-(4-Nitrobenzyl)-6-thioinosine (NBMPR), were purchased from Sigma.

Statistical analysis

Results are presented as mean of independent data points ± standard error of the mean (SEM). Number of neurons was used as a sample size for electrophysiology comparisons (one neuron per slice), and number of slices for Ca^{2+} signal comparisons. Data normality was assessed using a Shapiro–Wilk statistical test. When data met normal distribution results were compared using a two-tailed Student's t-test (paired, before-after stimulus-treatment; unpaired between groups). Otherwise, data were compared using a Mann-Whitney test. Statistical differences were established with $p < 0.05$ (*), $p < 0.01$ (**) and $p < 0.001$ (***). Details on sample size and statistical testing are provided in the Figure legends.

RESULTS

Glucose-deprived conditions depress synaptic transmitter release via nucleotide hydrolysis and activation of presynaptic adenosine receptors

To investigate the effects of glucose deprivation on synaptic transmission, we performed whole-cell patch-clamp recordings of CA1 pyramidal neurons and monitored EPSCs evoked by electrical stimulation of the Schaffer collaterals (SC) in hippocampal slices. The amplitude of EPSCs progressively declined during glucose deprivation (10-minute-long perfusion with 0 glucose ACSF), reaching a minimum of 77.9 ± 4.8% (n = 11) relative to basal (Figs. 1A,D). This reduction in the size of evoked EPSCs was fully restored following washout with glucose-containing ACSF. Notably, the presence of 1 µM CPT, a selective antagonist of adenosine A1 receptors, prevented the suppression of evoked EPSC induced by glucose deprivation (101.0 ± 4.8% of control values; n = 6; Figs. 1A,D).

To assess whether the effects of glucose deprivation on synaptic transmission were mediated pre- or postsynaptically, we evaluated changes in paired-pulse facilitation, a parameter indicative of presynaptic function [29]. The PPR exhibited a significant increase from 0.33 ± 0.11 under control conditions to 0.47 ± 0.12 in the absence of glucose (Figs. 1B,C; n = 8). This shift in PPR suggests that a reduced presynaptic probability of neurotransmitter release is the primary mechanism underlying the observed suppression of excitatory transmission. These findings, which are consistent with previous reports [27, 29, 30], indicate that synaptic depression induced by glucose deprivation is specifically mediated by presynaptic adenosine A1 receptors.

Adenosine can be synthesized intracellularly and subsequently transported out of the cell via equilibrative nucleoside transporters (ENTs) [31, 32] or generated extracellularly through the enzymatic hydrolysis of nucleotides by ecto-5′-nucleotidases [33]. ENTs facilitate

bidirectional, passive diffusion of adenosine across cell membranes, driven by its concentration gradient between the intra- and extracellular compartments [34]. Under physiological conditions, these transporters primarily mediate adenosine uptake from the extracellular space, but they have been also implicated in its release from neurons and astrocytes [35, 36]. To determine the role of nucleoside transport in glucose deprivation-induced synaptic depression, we used the adenosine transport inhibitors dipyridamole (DPM; 10 μM) and nitrobenzylthioinosine (NBMPR; 10 μM) [37]. Glucose deprivation continued to depress synaptic transmission in the presence of DPM and NBMPR (Fig. 1D; n = 6), arguing against direct adenosine release as a mechanism underlying the suppression of excitatory transmission. To further explore the underlying processes, we examined the effect of inhibiting ecto-5′-nucleotidases using ARL67156 [38, 39]. Notably, ARL67156 (50 μM) effectively prevented synaptic depression during glucose deprivation (101.0 ± 7.5% from basal; Fig. 1D; n = 9). Collectively, these findings indicate that the suppression of synaptic transmission induced by glucose deprivation in the CA1 region of the hippocampus is primarily mediated by the extracellular metabolism of adenine nucleotides leading to adenosine, rather than by direct adenosine transport. This extracellularly-generated adenosine subsequently activates presynaptic A1 receptors to depress excitatory synaptic transmission.

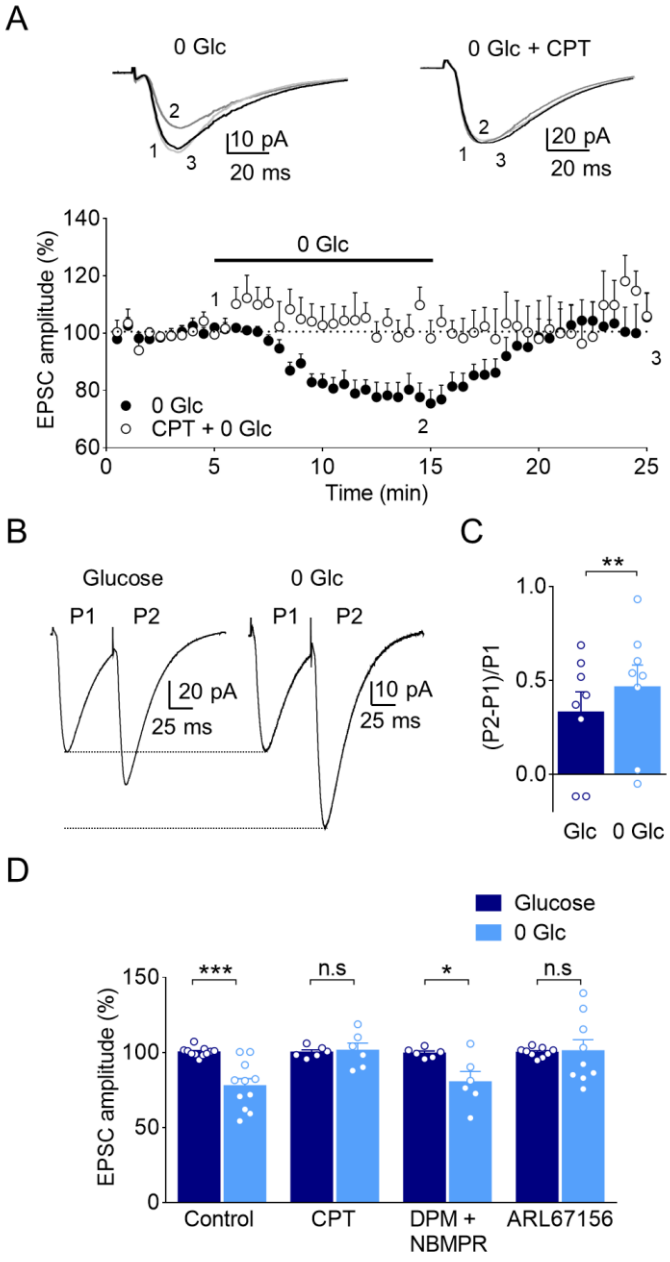

Figure 1. The absence of glucose decreases EPSC amplitude via a presynaptic mechanism involving adenosine. **(A)** The effect of glucose deprivation on normalized mean EPSC amplitudes induced by Schaffer collateral (SC) stimulation over time is shown for control conditions (filled circles, n = 11 neurons/slices from 4 mice) and in the presence of 1 μM CPT (open circles, n = 6 neurons/slices from 3 mice). The inset displays averaged EPSCs recorded before (1), during (2), and after (3) glucose deprivation, with or without CPT. **(B)** Averaged EPSCs triggered by paired-pulse stimulation (50 ms delay) are shown for glucose ACSF and 0 glucose conditions. Under 0 glucose, EPSCs were rescaled so that the first EPSC matched the size observed in glucose and 0 glucose conditions. **(C)** Averaged PPR [(P2–P1)/P1] was significantly different (n = 8 neurons/slices from 3 mice; **p < 0.01) in glucose and 0 glucose. **(D)** Summary data of 0 glucose-induced EPSC reduction in control condition and in the presence of 1 μM CPT (n = 6 neurons/slices from 3 mice), 10 μM DPM plus 10 μM NBMPR (n = 6 neurons/slices from 2 mice), and 50 μM ARL67156 (n = 9 neurons/slices from 2 mice). Significant differences with respect to glucose were established at *p < 0.05, **p < 0.01 and ***p < 0.001.

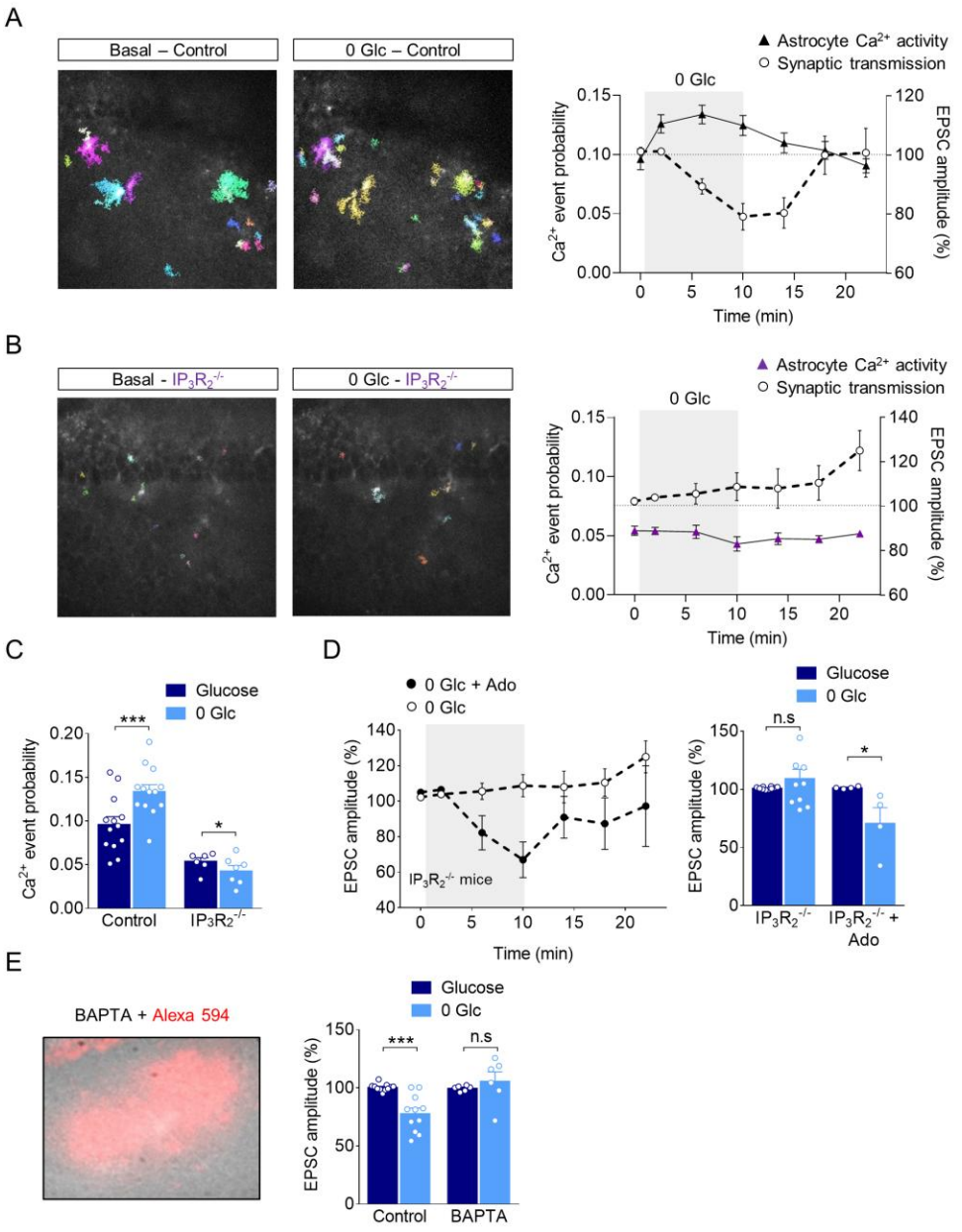

Figure 2. Glucose deprivation induced synaptic depression requires astrocytic calcium elevation. (A, B) *Left:* Representative images of astrocytic calcium events accumulated over a 2-minute period in acute hippocampal slices from control (**A**) and $IP_3R2^{-/-}$ mice (**B**) under glucose ACSF and after 10 minutes of glucose deprivation. *Right:* Time course of glucose deprivation effects on astrocytic Ca^{2+} event probability (triangles, n = 13 for control; n = 7 for $IP_3R2^{-/-}$) and normalized mean EPSC amplitudes (circles, n = 11 neurons/slices from 4 mice; n = 10 neurons/slices from 2 mice for $IP_3R2^{-/-}$). **(C)** Quantification of astrocyte Ca^{2+} event probability in control (n = 13 slices from 3 mice) and $IP_3R2^{-/-}$ (n = 7 slices from 2 mice) slices before and after 10 minutes of glucose deprivation. **(D)** Time course (left) and quantification of relative changes (right) in normalized mean EPSC amplitudes during glucose deprivation alone (n = 10 neurons/slices from 2 mice) or in the presence of adenosine (20 μM, n = 4 neurons/slices from 2 mice) in $IP_3R2^{-/-}$ slices. **(E)** *Left:* Representative image of a patched astrocyte dialyzed with BAPTA and Alexa 594, showing the astrocyte syncytium. *Right:* Effect of glucose deprivation on normalized mean EPSC amplitudes in control (n = 11 neurons/slices from 4 mice) and BAPTA-loaded astrocyte network-containing slices (n = 6 neurons/slices from 2 mice). Significant differences with respect to glucose were established at *p < 0.05 and ***p < 0.001.

Glucose deprivation-induced synaptic depression depends on astrocyte Ca^{2+} signaling

Astrocytes modulate synaptic transmission through the release of gliotransmitters, with ATP being one of the most common ones [40–42]. Based on the above-mentioned observations, we hypothesized that the excitatory synaptic depression induced by glucose deprivation is mediated by ATP released from astrocytes and subsequently converted into adenosine. Since Ca^{2+}-dependent processes are a major mechanism of gliotransmitter release [43–45], we next performed confocal imaging of GCaMP6f in hippocampal slices to investigate whether glucose deprivation modulates the astrocyte Ca^{2+} signal. Under normal glucose conditions, spontaneous astrocyte Ca^{2+} activity quantified as Ca^{2+} event probability was 0.10 ± 0.01. This activity markedly increased to 0.13 ± 0.01 following 10 min of glucose deprivation (Figs. 2A,C; n = 13). Additionally, the duration of Ca^{2+} transients was prolonged, with the event half-with increasing from 5.39 ± 0.17 sec to 5.87 ± 0.22 sec (n = 13; Supplementary Figs. 1A,B). Notably, the time-course of this increase in the frequency and duration of the astrocyte Ca^{2+} events closely mirrored the progression of synaptic depression during glucose deprivation (Fig. 2A), which suggests a link between deregulation of astrocyte Ca^{2+} dynamics and synaptic activity under these conditions. Thus, we next asked if an increase of astrocyte Ca^{2+} activity is needed to produce the synaptic depression in glucose-deprived conditions. To address this, we used transgenic mice lacking inositol-1,4,5-trisphosphate (IP3)-receptor type 2 ($IP_3R_2^{-/-}$ mice), in which G protein-mediated astrocyte Ca^{2+} signal is largely impaired [46–48]. Glucose deprivation induced a small but significant decrease of the astrocyte Ca^{2+} event probability in hippocampal slices from $IP_3R_2^{-/-}$ mice (from 0.05 ± 0.01 to 0.04 ± 0.01;n = 7; Figs. 2B,C) and did not modulate the duration of Ca^{2+} events (from 5.45 ± 0.20 s to 5.79 ± 0.41s; n = 7; Supplementary Fig. 1A,B), in contrast to the increase observed in slices from control animals (Fig. 2A). Importantly, hippocampal synaptic transmission in $IP_3R_2^{-/-}$ mice remained unaffected during the glucose deprivation period (EPSC amplitude from 101.0 ± 0.4% to 109.0 ± 7.9%; n = 10), suggesting that the observed synaptic depression requires astrocyte responses mediated by the Ca^{2+} signaling (Figs. 2B,D). We next tested if adenosine receptor activation effectively produces synaptic depression in transgenic mice. Bath application of adenosine (20 μM) for 10 min resulted in a significant depression of EPSCs (from 101.0 ± 0.5% to 64.2 ± 9.8%; n = 4), thus indicating that A1 receptor-mediated presynaptic signaling is not compromised in the $IP_3R_2^{-/-}$ mice (Fig. 2D).

To further test the role of astrocytic Ca^{2+} signaling in synaptic regulation induced during glucose deprivation, we selectively chelated intracellular Ca^{2+} by injecting astrocytes with the fast, high-affinity Ca^{2+}-chelating molecule BAPTA [49–51]. During whole-cell recording from CA1 pyramidal neurons, an astrocyte in *stratum radiatum* was contacted with a patch electrode containing high (20 mM) concentrations of BAPTA in whole-cell configuration to enable BAPTA diffusion into the astrocyte. The patch pipette also contained Alexa 594 (100 μM), which enabled visualization of the astrocyte syncytium covering an area ~100 μm in diameter (Fig. 2E). Remarkably, following 20 min of astrocyte dialysis with 20 mM BAPTA, synaptic transmission was unaffected by 10 min of glucose deprivation (from 99.6 ± 0.9% to 106.0 ± 7.9%; n = 6; Fig. 2E). These observations confirm that endogenous Ca^{2+} activity in astrocytes is necessary for the depression of excitatory transmission induced by glucose deprivation in the CA1 region of the hippocampus.

In summary, these results suggest that glucose deprivation triggers astrocyte Ca^{2+} signaling potentially inducing the release of ATP, which, after being converted to adenosine, leads to presynaptic A_1 receptor activation and excitatory synaptic depression.

Glucose deprivation-induced hippocampal synaptic depression depends on astrocytic glucose sensing

Brain glucose supply relies mainly on GLUT1, which is expressed both in blood vessel endothelial cells and astrocytes [5, 52], and plays a crucial role in glucose sensing [53, 54]. Thus, we next investigated whether astrocytic GLUT1 mediates excitatory synaptic depression induced by glucose deprivation. With this aim, $GLUT1^{fl/fl}$ mice were locally injected with AAV8-GFAP-mCherry-Cre to selectively deplete GLUT1 expression in CA1 hippocampal astrocytes (Fig. 3A). Immuno-fluorescence analysis of GFAP and mCherry confirmed that these mice, herein termed $aGLUT1^{-/-}$, showed astrocytic selectivity of the virus expression (Fig. 3A) and high recombination efficiency (81.12 ± 5.77% $GFAP^+mCherry^+/GFAP^+$ cells; n = 4 mice) within the site of injection [54].

Imaging of GCaMP6f in hippocampal slices revealed an increased basal astrocytic Ca^{2+} activity in $aGLUT1^{-/-}$ mice compared to control animals (Ca^{2+} event probability: 0.13 ± 0.01 in $aGLUT1^{-/-}$ *vs* 0.1 ± 0.01 in control; n = 13; Fig. 3B-D). Additionally, the basal Ca^{2+} event duration was significantly longer in $aGLUT1^{-/-}$ compared to control mice (6.28 ± 0.32 sec vs 5.39 ± 0.17 sec; n = 13; Supplementary Fig 1A,B). However, when hippocampal slices from $aGLUT1^{-/-}$ mice were subjected to 10 min of glucose deprivation, the characteristic increases in

astrocytic Ca^{2+} event probability observed in slices from control mice were completely absent (Ca^{2+} event probability: to 0.117 ± 0.007; Fig. 3B-D). Similarly, synaptic transmission in aGLUT1$^{-/-}$ slices remained unaffected during glucose deprivation, with no reduction in EPSC amplitude (from 101.0 ± 1.3% to 102.0 ± 6.3%; n = 11), in contrast to the marked suppression observed in control slices (Fig. 3E). To ensure that the lack of synaptic depression in aGLUT1$^{-/-}$ slices was not due to an impairment in neuronal adenosine receptor function, we bath applied exogenous adenosine (20 µM) for 10 min. As expected, adenosine perfusion produced a robust inhibition of synaptic transmission with EPSC amplitude decreasing to 57.2 ± 11.4% (n = 6) (Fig. 3E). These results indicate that neuronal A1 adenosine receptors remain fully functional in aGLUT1$^{-/-}$ mice. Further analysis of evoked synaptic responses showed similar input–output curves, PPR and synaptic fatigue in neurons from aGLUT1$^{-/-}$ mice and control mice (Supplementary Fig. 2A-C), suggesting that astrocytic GLUT1 depletion does not lead to impairments in the basic synaptic properties within hippocampal CA1 region. Taken together, these data indicate that astrocytic GLUT1 is essential for both the Ca^{2+} response and the subsequent synaptic depression induced by glucose deprivation and underscore the role of astrocytes in translating glucose availability into the modulation of synaptic transmission via GLUT1.

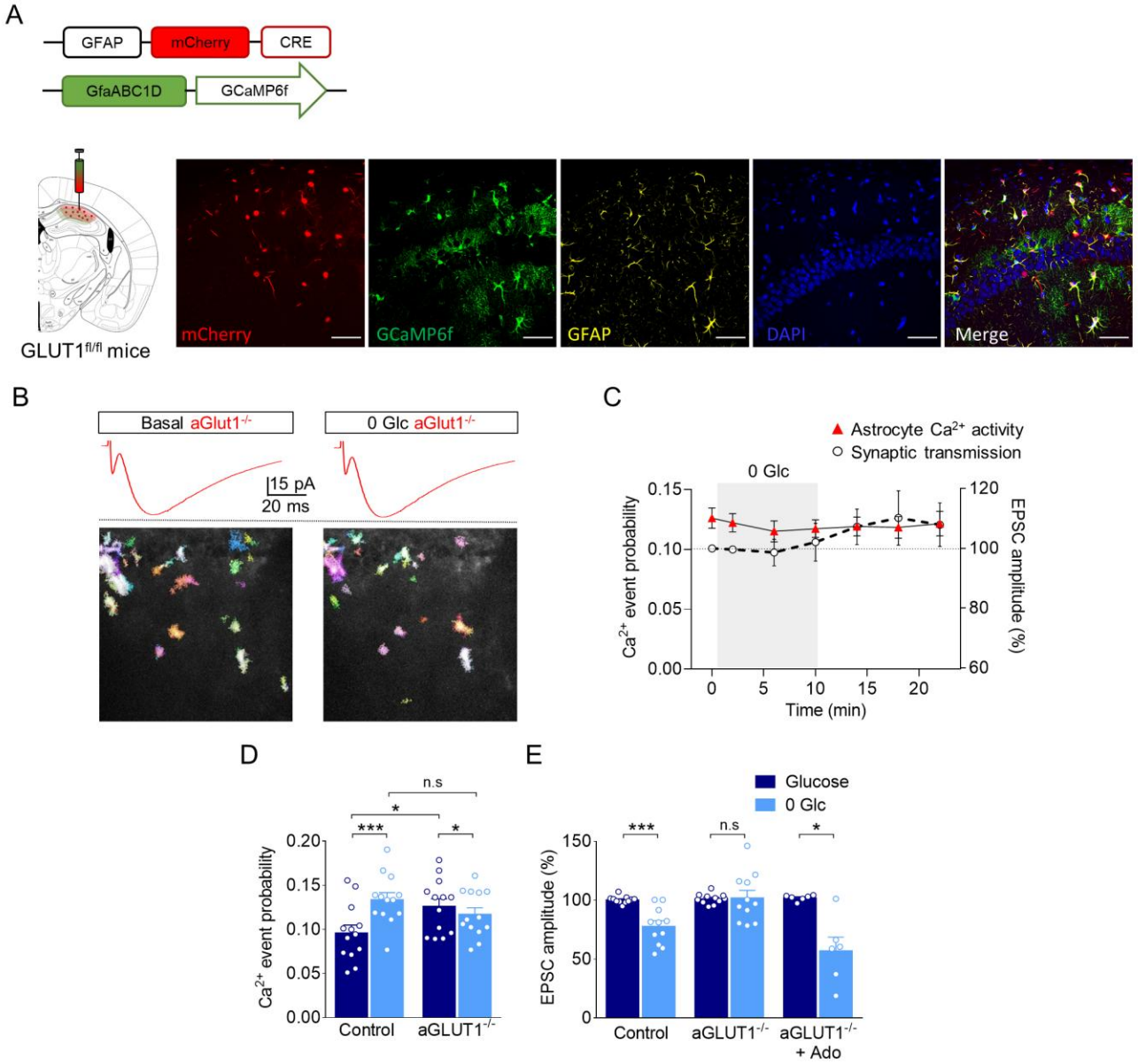

Figure 3. Astrocytic GLUT1 is required for glucose deprivation-induced synaptic depression. (A) *Left:* Schematic representation of AAV injections in hippocampal CA area of GLUT1$^{fl/fl}$ mice to abolish GLUT1 expression in astrocytes (aGLUT1$^{-/-}$). *Right:* representative confocal micrographs depict GCaMP6f fluorescence and immunolabeling of mCherry^{+} cells co-stained with GFAP and DAPI. Scale bar: 50 µm. **(B)** Representative traces of EPSCs and images of astrocytic calcium events accumulated over a 2-minute period in acute hippocampal slices from aGLUT1$^{-/-}$ mice under glucose ACSF and after 10 minutes of glucose deprivation. **(C)** Time course of glucose deprivation effects on astrocytic Ca^{2+} event probability (triangles) and normalized mean EPSC amplitudes (circles) in aGLUT1$^{-/-}$ mice. **(D)** Quantification of astrocyte Ca^{2+} event probability in control (n = 13 slices from 3 mice) and aGLUT1$^{-/-}$ (n = 13 slices from 4 mice) before and after 10 minutes of glucose deprivation. **(E)** Effect of glucose deprivation on normalized mean EPSC amplitudes in control (n = 11 neurons/slices from 4 mice), aGLUT1$^{-/-}$ (n = 11 neurons/slices from 4 mice) and aGLUT1$^{-/-}$ slices treated with adenosine (20 µM, n = 6 neurons/slices from 3 mice). Significant differences with respect to glucose were established at *p < 0.05 and ***p < 0.001.

DISCUSSION

Brain adaptation to metabolic challenge is a fundamental process that secures information processing and survival. Although glial cells play a prominent role in brain energy metabolism [55], how they cope with metabolic deficiency remains poorly understood. Our results show that glucose deprivation suppresses hippocampal excitatory transmission via an astrocyte-dependent mechanism that involves decreased GLUT1-mediated extracellular glucose uptake, Ca^{2+} signaling, and increased adenosine availability leading to the activation of presynaptic A1 receptors. These findings identify a novel role for astrocytic glucose uptake in modulating network responses to glucose deprivation and highlight the essential contribution of astroglial networks in maintaining metabolic homeostasis under conditions of energy scarcity. The combination of these features has led to the proposal that astrocytes act as converters of glucose availability information into synaptic transmission interventions [56].

While depression of hippocampal synaptic transmission during glucose deprivation has long been attributed to neuronal energy shortage, our results reveal an unexpected mechanism: astrocytic activity is the main driver of synaptic inhibition, even as neuronal firing persists. Indeed, our results demonstrate that astrocytes encode glucose deprivation, meaning that their activity reflects fluctuations in extracellular energy source availability. Specifically, glucose deprivation-induced hippocampal synaptic depression is dependent on astrocytic glucose sensing and Ca^{2+} activity translated into gliotransmitter release. These findings challenge the traditional neuronal metabolism-centered view and implicate glial signaling rather than direct neuronal metabolic failure in glucose-deprived conditions.

Elevation of astrocytic Ca^{2+} levels during glucose deprivation has been proposed to regulate synaptic transmission through multiple mechanisms [57]. This response may facilitate glycogenolysis, as previously demonstrated in human astrocytoma cells [58], thereby providing a local glucose supply to sustain neuronal activity. Alternatively, increased astrocytic Ca^{2+} signaling may contribute to energy conservation by actively downregulating synaptic efficacy via gliotransmitter release, particularly ATP. Extracellular ATP is rapidly converted into adenosine, which, by activating presynaptic A1 receptors, suppresses glutamate release and synaptic transmission [38]. Our findings support this model by showing that synaptic depression induced by presynaptic adenosine A1 receptors require both astrocytic GLUT1 and Ca^{2+}activity, further implicating astrocytes in metabolic adaptations to glucose-limiting conditions.

Previous studies have reported astrocytic Ca^{2+} elevations in response to glucose deprivation in the nucleus tractus solitarius (NTS), a brain region implicated in glucose sensing and homeostasis [59]. NTS astrocytes exhibit a reversible Ca^{2+} increase upon glucose withdrawal and restoration, leading to their classification as putative glucosensors alongside ventromedial hypothalamic neurons, which are either excited (GE neurons) or inhibited (GI neurons) by glucose [60]. Furthermore, inhibition of NTS astrocytes disrupts gastric vagal reflex circuits and motility during glucose deprivation, underscoring their functional importance in metabolic regulation [61]. Another study further extended this concept, as electrophysiological recordings of hippocampal astroglial cells in the *stratum radiatum* revealed that glucose shortage specifically increased astrocyte membrane capacitance, while having no impact on other passive membrane properties [57]. Consistent with this change, morphometric analysis unraveled a prompt increase in astrocyte volume upon glucose deprivation. Furthermore, the functional properties of astrocytes were also affected by transient glucose deficiency: glucose deprivation decreased gap junction-mediated coupling, while progressively and reversibly increasing intracellular Ca^{2+} levels during the slow depression of synaptic transmission that occurred simultaneously, as assessed by dual electrophysiological and Ca^{2+} imaging recordings [57]. Our study extends this idea by demonstrating that astrocytes outside canonical glucose-sensing regions also respond to changes in glucose availability and therefore suggest that astrocytic

glucosensing is a widespread and fundamental property of brain energy homeostasis.

A key and novel observation in our study is that hippocampal astrocytes from aGLUT1$^{-/-}$ mice fail to increase Ca^{2+} activity in response to glucose deprivation, indicating that astrocytic GLUT1-dependent glucose uptake is necessary for this response. This lack of astrocyte Ca^{2+} responsiveness likely results from elevated basal Ca^{2+} signaling, which precludes further increases upon glucose deprivation. These findings indicate that astrocytic glucose uptake and subsequent metabolization are a prerequisite for their ability to detect and respond to metabolic fluctuations. When astrocytes are unable to import and metabolize glucose, the entire circuit ceases to adapt to extracellular glucose deprivation, reinforcing the notion that astrocytic sensitivity to glucose fluctuations is an essential component of brain metabolic regulation and synaptic transmission modulation [54].

Limitations of the study

While in this study we used a complete glucose deprivation paradigm to clearly elucidate the fundamental mechanisms by which astrocytic glucose sensing influences synaptic regulation, it is important to consider the physiological relevance of the present findings in the context of more subtle glucose fluctuations. *In vivo* brain glucose levels, particularly within the CSF, typically reside in the 3-4 mM range in humans [62–64]. However, even within this physiological range, and during conditions of mild glucose deprivation, astrocytes are exquisitely sensitive to changes in glucose availability [65, 66]. Therefore, our findings, although derived from an experimental manipulation that does not fully mimic *in vivo* glucose shortages, most likely highlight fundamental pathways that are engaged and modulate synaptic function even under less severe, physiologically relevant alterations in glucose supply, and potentially contribute to the synaptic plasticity observed during various metabolic states or in the context of neurological disorders involving impaired glucose metabolism.

Another limitation that warrants further consideration is the intriguing possibility of sex-specific differences in astrocyte responses upon glucose deprivation. While our current investigation provides fundamental insights into the general mechanisms by which astrocytic glucose sensing regulates synaptic activity, emerging evidence highlights that astrocytes exhibit sex-dependent variations in their molecular profiles and functional responses [67]. These inherent biological distinctions could translate into differential astrocytic reactions to glucose deprivation in males versus females, potentially leading to distinct modulatory effects on synaptic circuits. Given the well-documented sex biases observed in the prevalence and severity of numerous neurological disorders characterized by metabolic dysfunction, such as Alzheimer's disease (AD), stroke, and epilepsy, future studies specifically designed to investigate these sex-dependent astrocytic responses to glucose availability and their subsequent impact on synaptic function are crucial. Unraveling these potential sex-specific mechanisms could offer valuable insights into the differential vulnerability and resilience of the sexes to these neurological conditions and pave the way for more personalized therapeutic interventions.

Conclusion

Our study establishes a direct link between astrocyte glucose uptake and neuromodulation by demonstrating that synaptic depression mediated by adenosine A1 receptors depends on astrocytic GLUT1 and Ca^{2+} activity. The abolition of astrocytic Ca^{2+} responses to glucose deprivation in aGLUT1$^{-/-}$ mice further highlights GLUT1 as a key participant in astrocytic glucosensing [54]. Mechanistically, our findings suggest that ATP release and its subsequent conversion to adenosine underlie astrocyte-dependent synaptic depression during glucose deprivation. These results emphasize the critical role of astrocytic glucose uptake in adapting to metabolic stress and regulating neuronal function under hypoglycemic conditions. Moreover, the present observations have significant implications for pathological states associated with glucose deficiency, such as GLUT1 deficiency syndrome [68] and AD [69], where GLUT1 downregulation contributes to neurodegeneration. By elucidating how astrocytes sense and respond to metabolic challenges, our study highlights potential therapeutic targets for disorders characterized by impaired brain energy metabolism. Future research should explore how astrocytic metabolic networks adapt to chronic metabolic stress and whether modulating astrocytic glucose uptake could provide neuroprotective strategies.

Acknowledgements

We would like to thank the personnel of the Animal Facilities of University of Minnesota and the University of Navarra for mouse care. This work was funded by MICIU/AEI/10.13039/501100011033 and by "ERDF A way of making Europe" (SAF2017-87619-P and PID2021-128737NB-I00) to M.S., the Instituto de Salud Carlos III cofunded by the European Union (PI21/00629, to S.M.) the Basque Government (PIBA_2023_1_0046; 2023111031; IT1473-22 to S.M.), ARSEP Foundation (ARSEP-1310 to S.M.), the Postdoctoral Program of the Basque Government (to A.M.B.), a Formación de Profesorado Universitario (FPU) fellowship and an associated Mobility grant from the Spanish Ministry of

Universities (FPU18/01458 and EST21/00300, respectively, to C.G.A.), and grants from National Institutes of Health (NIH-NIMH R01MH119355 and NIH-NIDA R01DA048822) and Department of Defense (W911NF2110328) to A.A.

Supplementary Materials

The Supplementary data can be found online at: www.aginganddisease.org/EN/10.14336/AD.2025.0507.

References

[1] Bonvento G, Bolaños JP (2021). Astrocyte-neuron metabolic cooperation shapes brain activity. Cell Metabolism, 33:1546–1564.

[2] Bélanger M, Allaman I, Magistretti PJ (2011). Brain energy metabolism: focus on astrocyte-neuron metabolic cooperation. Cell Metab, 14:724–738.

[3] Kacem K, Lacombe P, Seylaz J, Bonvento G (1998). Structural organization of the perivascular astrocyte endfeet and their relationship with the endothelial glucose transporter: a confocal microscopy study. Glia, 23:1–10.

[4] Mathiisen TM, Lehre KP, Danbolt NC, Ottersen OP (2010). The perivascular astroglial sheath provides a complete covering of the brain microvessels: an electron microscopic 3D reconstruction. Glia, 58:1094–1103.

[5] Hösli L, Zuend M, Bredell G, Zanker HS, Porto de Oliveira CE, Saab AS, et al. (2022). Direct vascular contact is a hallmark of cerebral astrocytes. Cell Rep, 39:110599.

[6] Pellerin L, Magistretti PJ (1994). Glutamate uptake into astrocytes stimulates aerobic glycolysis: a mechanism coupling neuronal activity to glucose utilization. Proc Natl Acad Sci U S A, 91:10625–10629.

[7] Ardanaz CG, Ramírez MJ, Solas M (2022). Brain Metabolic Alterations in Alzheimer's Disease. International Journal of Molecular Sciences, 23:3785.

[8] Araque A, Parpura V, Sanzgiri RP, Haydon PG (1999). Tripartite synapses: glia, the unacknowledged partner. Trends Neurosci, 22:208–215.

[9] Perea G, Araque A (2007). Astrocytes potentiate transmitter release at single hippocampal synapses. Science, 317:1083–1086.

[10] Perea G, Navarrete M, Araque A (2009). Tripartite synapses: astrocytes process and control synaptic information. Trends Neurosci, 32:421–431.

[11] Wender R, Brown AM, Fern R, Swanson RA, Farrell K, Ransom BR (2000). Astrocytic glycogen influences axon function and survival during glucose deprivation in central white matter. J Neurosci, 20:6804–6810.

[12] Brown AM (2004). Brain glycogen re-awakened. J Neurochem, 89:537–552.

[13] Brown AM, Sickmann HM, Fosgerau K, Lund TM, Schousboe A, Waagepetersen HS, et al. (2005). Astrocyte glycogen metabolism is required for neural activity during aglycemia or intense stimulation in mouse white matter. J Neurosci Res, 79:74–80.

[14] Mergenthaler P, Lindauer U, Dienel GA, Meisel A (2013). Sugar for the brain: the role of glucose in physiological and pathological brain function. Trends Neurosci, 36:587–597.

[15] Papadopoulos MC, Koumenis IL, Dugan LL, Giffard RG (1997). Vulnerability to glucose deprivation injury correlates with glutathione levels in astrocytes. Brain Res, 748:151–156.

[16] Ioudina M, Uemura E, Greenlee HW (2004). Glucose insufficiency alters neuronal viability and increases susceptibility to glutamate toxicity. Brain Res, 1004:188–192.

[17] Harris JJ, Jolivet R, Attwell D (2012). Synaptic energy use and supply. Neuron, 75:762–777.

[18] Howarth C, Gleeson P, Attwell D (2012). Updated energy budgets for neural computation in the neocortex and cerebellum. J Cereb Blood Flow Metab, 32:1222–1232.

[19] Korol DL, Gold PE (1998). Glucose, memory, and aging. Am J Clin Nutr, 67:764S-771S.

[20] Abdelhafiz AH, Rodríguez-Mañas L, Morley JE, Sinclair AJ (2015). Hypoglycemia in older people - a less well recognized risk factor for frailty. Aging Dis, 6:156–167.

[21] McNay EC, Gold PE (2001). Age-related differences in hippocampal extracellular fluid glucose concentration during behavioral testing and following systemic glucose administration. J Gerontol A Biol Sci Med Sci, 56:B66-71.

[22] Syková E (2001). Glial diffusion barriers during aging and pathological states. Prog Brain Res, 132:339–363.

[23] Syková E, Mazel T, Hasenöhrl RU, Harvey AR, Simonová Z, Mulders WH a. M, et al. (2002). Learning deficits in aged rats related to decrease in extracellular volume and loss of diffusion anisotropy in hippocampus. Hippocampus, 12:269–279.

[24] McNay EC (2005). The impact of recurrent hypoglycemia on cognitive function in aging. Neurobiol Aging, 26 Suppl 1:76–79.

[25] Rouach N, Koulakoff A, Abudara V, Willecke K, Giaume C (2008). Astroglial metabolic networks sustain hippocampal synaptic transmission. Science, 322:1551–1555.

[26] Fernandez AM, Hernandez-Garzón E, Perez-Domper P, Perez-Alvarez A, Mederos S, Matsui T, et al. (2017). Insulin Regulates Astrocytic Glucose Handling Through Cooperation With IGF-I. Diabetes, 66:64–74.

[27] Kawamura M, Ruskin DN, Masino SA (2019). Adenosine A1 receptor-mediated protection of mouse hippocampal synaptic transmission against oxygen and/or glucose deprivation: a comparative study. J Neurophysiol, 122:721–728.

[28] Navarrete M, Araque A (2010). Endocannabinoids potentiate synaptic transmission through stimulation of astrocytes. Neuron, 68:113–126.

[29] Martín ED, Buño W (2003). Caffeine-mediated presynaptic long-term potentiation in hippocampal CA1 pyramidal neurons. J Neurophysiol, 89:3029–3038.

[30] Martín ED, Fernández M, Perea G, Pascual O, Haydon PG, Araque A, et al. (2007). Adenosine released by astrocytes contributes to hypoxia-induced modulation of synaptic transmission. Glia, 55:36–45.
[31] Higgins MJ, Hosseinzadeh H, MacGregor DG, Ogilvy H, Stone TW (1994). Release and actions of adenosine in the central nervous system. Pharm World Sci, 16:62–68.
[32] Boison D, Chen J-F, Fredholm BB (2010). Adenosine signaling and function in glial cells. Cell Death Differ, 17:1071–1082.
[33] Dunwiddie TV, Diao L, Proctor WR (1997). Adenine nucleotides undergo rapid, quantitative conversion to adenosine in the extracellular space in rat hippocampus. J Neurosci, 17:7673–7682.
[34] Noji T, Karasawa A, Kusaka H (2004). Adenosine uptake inhibitors. Eur J Pharmacol, 495:1–16.
[35] Bender AS, Hertz L (1986). Similarities of adenosine uptake systems in astrocytes and neurons in primary cultures. Neurochem Res, 11:1507–1524.
[36] Brundege JM, Dunwiddie TV (1996). Modulation of excitatory synaptic transmission by adenosine released from single hippocampal pyramidal neurons. J Neurosci, 16:5603–5612.
[37] Dunwiddie TV, Diao L (2000). Regulation of extracellular adenosine in rat hippocampal slices is temperature dependent: role of adenosine transporters. Neuroscience, 95:81–88.
[38] Pascual O, Casper KB, Kubera C, Zhang J, Revilla-Sanchez R, Sul J-Y, et al. (2005). Astrocytic purinergic signaling coordinates synaptic networks. Science, 310:113–116.
[39] Lévesque SA, Lavoie EG, Lecka J, Bigonnesse F, Sévigny J (2007). Specificity of the ecto-ATPase inhibitor ARL 67156 on human and mouse ectonucleotidases. Br J Pharmacol, 152:141–150.
[40] Araque A, Carmignoto G, Haydon PG (2001). Dynamic signaling between astrocytes and neurons. Annu Rev Physiol, 63:795–813.
[41] Bezzi P, Volterra A (2001). A neuron-glia signalling network in the active brain. Curr Opin Neurobiol, 11:387–394.
[42] Haydon PG (2001). GLIA: listening and talking to the synapse. Nat Rev Neurosci, 2:185–193.
[43] Araque A, Sanzgiri RP, Parpura V, Haydon PG (1998). Calcium elevation in astrocytes causes an NMDA receptor-dependent increase in the frequency of miniature synaptic currents in cultured hippocampal neurons. J Neurosci, 18:6822–6829.
[44] Goenaga J, Araque A, Kofuji P, Herrera Moro Chao D (2023). Calcium signaling in astrocytes and gliotransmitter release. Front Synaptic Neurosci, 15:1138577.
[45] Baraibar AM, Colomer T, Moreno-García A, Bernal-Chico A, Sánchez-Martín E, Utrilla C, et al. (2024). Autoimmune inflammation triggers aberrant astrocytic calcium signaling to impair synaptic plasticity. Brain Behav Immun, 121:192–210.
[46] Petravicz J, Fiacco TA, McCarthy KD (2008). Loss of IP3 receptor-dependent Ca2+ increases in hippocampal astrocytes does not affect baseline CA1 pyramidal neuron synaptic activity. J Neurosci, 28:4967–4973.
[47] Di Castro MA, Chuquet J, Liaudet N, Bhaukaurally K, Santello M, Bouvier D, et al. (2011). Local Ca2+ detection and modulation of synaptic release by astrocytes. Nat Neurosci, 14:1276–1284.
[48] Baraibar AM, Belisle L, Marsicano G, Matute C, Mato S, Araque A, et al. (2023). Spatial organization of neuron-astrocyte interactions in the somatosensory cortex. Cereb Cortex, 33:4498–4511.
[49] Serrano A, Haddjeri N, Lacaille J-C, Robitaille R (2006). GABAergic network activation of glial cells underlies hippocampal heterosynaptic depression. J Neurosci, 26:5370–5382.
[50] Panatier A, Vallée J, Haber M, Murai KK, Lacaille J-C, Robitaille R (2011). Astrocytes are endogenous regulators of basal transmission at central synapses. Cell, 146:785–798.
[51] Matos M, Bosson A, Riebe I, Reynell C, Vallée J, Laplante I, et al. (2018). Astrocytes detect and upregulate transmission at inhibitory synapses of somatostatin interneurons onto pyramidal cells. Nat Commun, 9:4254.
[52] Nguyen YTK, Ha HTT, Nguyen TH, Nguyen LN (2021). The role of SLC transporters for brain health and disease. Cell Mol Life Sci, 79:20.
[53] Camandola S (2018). Astrocytes, emerging stars of energy homeostasis. Cell Stress, 2:246–252.
[54] Ardanaz CG, de la Cruz A, Minhas PS, Hernández-Martín N, Pozo MÁ, Valdecantos MP, et al. (2024). Astrocytic GLUT1 reduction paradoxically improves central and peripheral glucose homeostasis. Sci Adv, 10:eadp1115.
[55] Ardanaz CG, Ramírez MJ, Solas M (2022). Brain Metabolic Alterations in Alzheimer's Disease. Int J Mol Sci, 23:3785.
[56] Rogers RC, Burke SJ, Collier JJ, Ritter S, Hermann GE (2020). Evidence that hindbrain astrocytes in the rat detect low glucose with a glucose transporter 2-phospholipase C-calcium release mechanism. Am J Physiol Regul Integr Comp Physiol, 318:R38–R48.
[57] Lee C-Y, Dallérac G, Ezan P, Anderova M, Rouach N (2016). Glucose Tightly Controls Morphological and Functional Properties of Astrocytes. Front Aging Neurosci, 8:82.
[58] Medrano S, Gruenstein E, Dimlich RV (1992). Histamine stimulates glycogenolysis in human astrocytoma cells by increasing intracellular free calcium. Brain Res, 592:202–207.
[59] McDougal DH, Hermann GE, Rogers RC (2013). Astrocytes in the nucleus of the solitary tract are activated by low glucose or glucoprivation: evidence for glial involvement in glucose homeostasis. Front Neurosci, 7:249.
[60] Pénicaud L, Leloup C, Fioramonti X, Lorsignol A, Benani A (2006). Brain glucose sensing: a subtle mechanism. Curr Opin Clin Nutr Metab Care, 9:458–462.
[61] Hermann GE, Viard E, Rogers RC (2014). Hindbrain glucoprivation effects on gastric vagal reflex circuits and

gastric motility in the rat are suppressed by the astrocyte inhibitor fluorocitrate. J Neurosci, 34:10488–10496.

[62] Marks V (1960). True glucose content of lumbar and ventricular cerebrospinal fluid. J Clin Pathol, 13:82–84.

[63] Lundquist I (1972). Interaction of amines and aminergic blocking agents with blood glucose regulation. I. Beta-adrenergic blockade. Eur J Pharmacol, 18:213–224.

[64] Nigrovic LE, Kimia AA, Shah SS, Neuman MI (2012). Relationship between cerebrospinal fluid glucose and serum glucose. N Engl J Med, 366:576–578.

[65] Pellerin L (2018). Neuroenergetics: Astrocytes Have a Sweet Spot for Glucose. Curr Biol, 28:R1258–R1260.

[66] Ardanaz CG, de la Cruz A, Minhas PS, Hernández-Martín N, Pozo MÁ, Valdecantos MP, et al. (2024). Astrocytic GLUT1 reduction paradoxically improves central and peripheral glucose homeostasis. Sci Adv, 10:eadp1115.

[67] Gozlan E, Lewit-Cohen Y, Frenkel D (2024). Sex Differences in Astrocyte Activity. Cells, 13:1724.

[68] Wang D, Pascual JM, Yang H, Engelstad K, Jhung S, Sun RP, et al. (2005). Glut-1 deficiency syndrome: clinical, genetic, and therapeutic aspects. Ann Neurol, 57:111–118.

[69] Winkler EA, Nishida Y, Sagare AP, Rege SV, Bell RD, Perlmutter D, et al. (2015). GLUT1 reductions exacerbate Alzheimer's disease vasculo-neuronal dysfunction and degeneration. Nat Neurosci, 18:521–530.